Optimization of CO_2 and H_2 Storage in Plastic-Derived Carbon Using Molecular Dynamics and GCMC

Mentors: Carla De Tomas · Jorge Anderson Arboleda

Norah Saad AlQarni

inorahsaad@gmail.com

Abstract

Nanoporous carbon can be made cheaply by heating waste plastic, which makes it an attractive material for storing hydrogen and for capturing carbon dioxide. This report asks a simple question about two such carbons, identical in chemistry but different in density (1.0 and 0.7 g cm^{-3}): *which one holds more gas, and why?*

Using grand canonical Monte Carlo combined with molecular dynamics in LAMMPS, we computed full adsorption isotherms for hydrogen at 77 K and partial isotherms for carbon dioxide at 273.15 K. Both materials give Type I isotherms in the IUPAC scheme, meaning gas fills tiny pores rather than coating surfaces. The answer to the question turns out to depend on pressure: the denser carbon wins when gas is scarce because it has more narrow, strongly binding pores, while the lighter carbon wins once those pores fill because it has more total space. For hydrogen the two swap places at a loading of about 11.9 mmol g^{-1}; the carbon dioxide runs stop just short of the equivalent crossover. We also measured something the project intended to correct for but ran out of time to implement: roughly a fifth to a third of the pore space in the denser carbon is *sealed off* from the outside, so simulated uptake counts gas that a real experiment could never load.

Date: August 2026

Correspondence: inorahsaad@gmail.com

A two-month project. The hydrogen study is complete; the carbon dioxide study was still running when this report was written, and the sections below say explicitly which conclusions are measured and which are provisional.

Contents

1 Introduction **2**

1.1 Why carbon made from plastic . . . 2

1.2 The question this project asks . . . 2

1.3 Two months, and what that meant . . . 2

2 The material **2**

2.1 What the carbon actually looks like . . . 3

2.2 Pore sizes . . . 3

3 How the simulations work **4**

3.1 Grand canonical Monte Carlo, in plain terms . . . 4

3.2 The models . . . 5

3.3 Getting honest error bars . . . 5

3.4 Why every plot uses relative pressure . . . 5

4 Hydrogen storage at 77 K **6**

4.1 The isotherms . . . 6

4.2 Checking the runs are trustworthy . . . 7

4.3 Two ways of reporting the same thing . . . 8

4.4 Where the hydrogen actually sits . . . 9

4.5 Full results . . . 10

5 Carbon dioxide capture at 273.15 K **11**

5.1 The pressure grid . . . 11

5.2 The isotherms . . . 12

5.3 Checking the runs . . . 13

5.4 Where the carbon dioxide sits . . . 15

5.5 Full results . . . 15

6 What the two gases show together **16**

6.1 Both materials give Type I isotherms . . . 16

6.2 How wide are the pores, really? . . . 17

6.3 Why the two carbons swap places . . . 19

7 Closed porosity: the piece we did not finish **19**

7.1 The problem . . . 20

7.2 What we intended to do in LAMMPS . . . 20

7.3 How much does it matter? A first measurement . . . 20

8 Limitations **21**

9 Conclusions **22**

Acknowledgements **22**

References **22**

1 Introduction

1.1 Why carbon made from plastic

Two of the most discussed problems in energy and climate research are how to store hydrogen compactly and how to capture carbon dioxide cheaply. Both are, at bottom, the same physical problem: you need a solid with an enormous internal surface that gas molecules will stick to.

Nanoporous carbon is one of the best candidates, and the interesting thing about it is where it can come from. Heating waste plastic without oxygen — pyrolysis — breaks the polymer down and leaves behind a carbon skeleton riddled with pores. Polyolefin waste is abundant, cheap, and notoriously difficult to recycle by any other route. A capture material whose raw ingredient is a waste stream inverts the usual economics, and it keeps plastic out of landfill and incinerators along the way.

Note

This report characterises the *structure* and the *gas uptake* of such a carbon. It does not measure synthesis yield, energy input, char purity, or life-cycle emissions, so nothing here proves the environmental case on its own. What the results support is the narrower and still useful claim that the pore structure this route produces is well suited to both jobs.

1.2 The question this project asks

We study two carbon frameworks with the same chemistry but different packing density: 1.0 and 0.7 $\mathrm{g\,cm^{-3}}$. Because they differ in only one property, comparing them isolates the effect of density cleanly. The guiding question is which density stores more gas per gram — and, more usefully, *why*, since the reason tells you how to design the next material rather than merely which of two samples to pick.

1.3 Two months, and what that meant

Attention

The project ran for two months. That was enough time to finish the hydrogen study completely, but not enough to finish the carbon dioxide study or to implement the closed-porosity correction described in Section 7. Roughly two thirds of the planned CO_2 simulations were still queued on the cluster when this report was written.

Simulations of this kind are slow. A single pressure point for carbon dioxide takes between four and sixteen hours on 40 processor cores, and the cost rises steeply with pressure because there are more molecules to track. The full plan was 17 pressure points for each density for each gas. Hydrogen finished. Carbon dioxide reached 9 of 17 points on the dense framework and 5 of 17 on the light one.

Rather than hide the gap, this report marks it everywhere it matters. Every CO_2 conclusion is labelled as measured or provisional, and Section 8 lists exactly what a continuation would need to run.

2 The material

2.1 What the carbon actually looks like

Both frameworks were built in OVITO and are cubes of amorphous carbon, repeated periodically so that a small box behaves like a piece of bulk material. The dense one holds 31,895 carbon atoms in an 86.08 Å cube; the light one holds 31,839 atoms in a 96.96 Å cube.

We checked the structures rather than trusting the filenames. Dividing mass by volume gives 0.997 and 0.697 g cm^{-3}, within 0.5% of nominal. Counting how many neighbours each carbon atom has shows that **97.9%** and **97.8%** of atoms have exactly three, and the average bond angle in both is **119.7°**. Three neighbours at 120° is the signature of graphite-like (sp^2) carbon. So these are not diamond-like networks: they are crumpled, defective graphene sheets packed at two different densities.

This kind of structure, and the way it is generated in simulation, has been studied in detail: the choice of interatomic potential strongly affects how an amorphous carbon graphitises and therefore what pore network it ends up with [1]. Carbons of this family can also be tuned across a range of densities while remaining chemically the same material [2], which is precisely the comparison this report exploits — two densities, one chemistry.

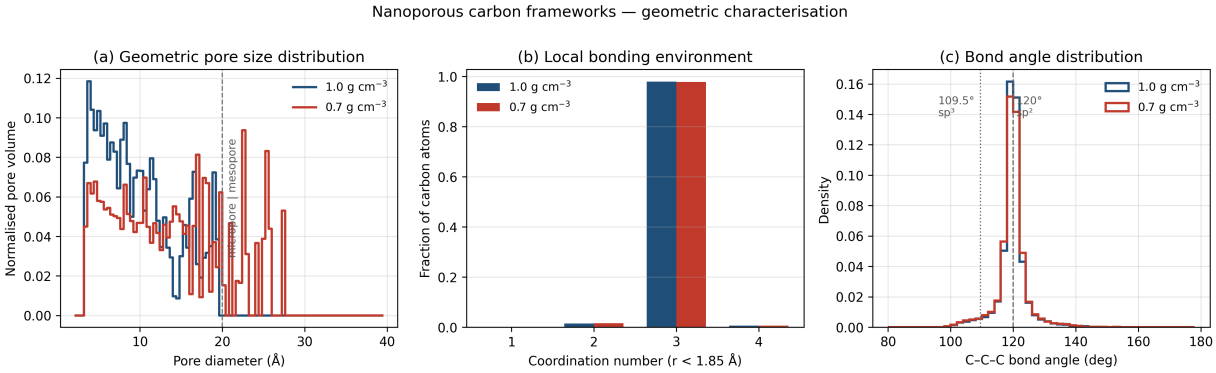


Figure 1 Geometric characterisation of the two frameworks. **(a)** Pore size distribution, with the 20 Å line that IUPAC uses to separate micropores from mesopores. The dense framework lies entirely to the left of it. **(b)** Number of neighbours per carbon atom — overwhelmingly three in both. **(c)** Bond angles, clustered on 120°, confirming sp^2 bonding.

2.2 Pore sizes

Pore sizes were measured geometrically: we ask, for every point in the empty space, how large a sphere could sit there without touching a carbon atom [3]. Carbon was given a radius of 1.715 Å, taken from the same force field the simulations use, so the geometry and the physics agree about how big an atom is.

Table 1 Framework properties. Void volume is the space a point-sized particle could occupy. Surface area uses a nitrogen-sized probe in the sense of Ref. [4], and is comparable to, but not identical with, an experimental BET measurement.

Property	1.0 g cm^{-3}	0.7 g cm^{-3}
Carbon atoms	31,895	31,839
Cube side	86.08 Å	96.96 Å
Measured density	0.997 g cm^{-3}	0.697 g cm^{-3}
Three-coordinate carbon	97.9%	97.8%
Mean bond angle	119.7°	119.7°
Most common pore diameter	3.8 Å	22.6 Å
Median pore diameter	8.8 Å	13.0 Å
Largest pore	19.4 Å	27.6 Å
Pore volume below 20 Å	100%	81%
Void volume	0.583 cm^3 g^{-1}	1.014 cm^3 g^{-1}
Surface area (N_2 probe)	1753 m^2 g^{-1}	2921 m^2 g^{-1}

Key Insight

The dense carbon is *entirely* microporous: even its largest pore, at 19.4 Å, sits under the 20 Å micropore ceiling. The light carbon reaches 27.6 Å and puts 19% of its volume into mesopores. It also has 74% more void space per gram. This single structural difference explains almost every result that follows.

3 How the simulations work

3.1 Grand canonical Monte Carlo, in plain terms

In an ordinary simulation you decide in advance how many molecules are in the box. That is useless here, because the number of molecules the carbon soaks up is exactly what we want to find out.

Grand canonical Monte Carlo (GCMC) solves this. It repeatedly proposes to insert a new gas molecule at a random position, or to delete one that is already there, and accepts or rejects each proposal according to a rule derived from statistical mechanics. The rule connects the box to an imaginary external gas reservoir held at the target pressure. Left to run, the number of molecules in the box drifts to whatever value equilibrium demands — which is the adsorbed amount we are after.

Between batches of insertion and deletion attempts, ordinary molecular dynamics (MD) lets the molecules already inside move around and settle into comfortable positions. The combination is what "GCMC/MD" means. Molecular dynamics is the standard tool for questions of this type, where the quantity of interest is how molecules arrange themselves against a solid surface [5, 6].

3.2 The models

Table 2 Simulation settings for both studies. The carbon framework is held rigid throughout, so the only thing that moves is the gas.

	Hydrogen study	Carbon dioxide study
Temperature	77 K	273.15 K
Molecule model	2 sites, rigid	3 sites, rigid (O–C–O 175°)
Site well depth	12.5 K per site	39.4 K (C), 112.7 K (O)
Site diameter	2.72 Å	2.120 Å (C), 2.330 Å (O)
Electric charges	none	none
Framework carbon	52.84 K, 3.43086 Å	52.84 K, 3.43086 Å
Interaction cutoff	16.55 Å	16.55 Å
Settling steps	3 000 000	1 000 000
Measurement steps	1 000 000	1 000 000
Pressure points	19 (complete)	17 planned, 12 run

The hydrogen molecule uses the standard two-site model of Cracknell [7], and the framework carbon takes its parameters from the UFF force field [8]; both were specified in the project files rather than chosen here. We verified the framework values by working backwards from the combined parameters given in the input and recovering $\sigma = 3.43086$ Å and $\epsilon/k_B = 52.84$ K, which are exactly the UFF carbon values.

Two further details are worth explaining. First, the carbon dioxide molecule is modelled with a 175° bend instead of being perfectly straight. This is not a physical choice: a perfectly linear rigid body has a mathematical degeneracy that the simulation code cannot handle when molecules are created and destroyed, and bending it by five degrees removes the problem without measurably changing the physics.

Second, neither molecule carries electric charges. For hydrogen that is standard and harmless. For carbon dioxide it is a real approximation, and Section 8 returns to it.

3.3 Getting honest error bars

Even at equilibrium the number of molecules in the box jitters, and readings taken close together in time resemble each other. Treating every reading as independent would make the error bars look far better than they really are.

Instead we group the readings into blocks, then blocks of blocks, until neighbouring blocks stop resembling one another; the spread between those blocks is the true uncertainty [9]. All uncertainties in this report are computed this way, and they run between 0.19% and 0.91% of the measured value.

3.4 Why every plot uses relative pressure

Adsorption results are conventionally plotted against *relative* pressure p/p_0 rather than absolute pressure, and every isotherm in this report follows that convention. The reason is that what governs the shape of an isotherm is how close the gas is to condensing, not how many bar the gauge reads. p_0 is the pressure at which the gas would liquefy at that temperature, so $p/p_0 = 1$ means saturation and $p/p_0 = 10^{-4}$ means very dilute. It is also the axis the IUPAC classification of Section 6 is defined on.

For carbon dioxide at 273.15 K this is straightforward: $p_0 = 34.851$ bar.

Note

Hydrogen at 77 K has no saturation pressure at all. Its critical temperature is 33.19 K, so at 77 K it is supercritical — no amount of pressure will liquefy it. Where a relative pressure is needed for hydrogen we use Dubinin's *pseudo*-saturation pressure, $p_0 = P_c(T/T_c)^2 = 69.78$ bar, and every hydrogen axis in this report is labelled "pseudo" to make that explicit. It allows the two gases to be compared on one axis, but it is a convention, not a physical boiling point.

4 Hydrogen storage at 77 K

This study is **complete**: 19 pressure points for each framework, covering seven decades from 10^{-6} to 100 bar.

4.1 The isotherms

An *isotherm* is simply a plot of how much gas the material holds against the pressure it is held at, all at one fixed temperature. Pressure is plotted here as *relative* pressure p/p_0, the convention in adsorption science, because it is how full the pores get — not the absolute pressure — that governs the shape of the curve. Section 3.4 explains where p_0 comes from for a supercritical gas like hydrogen.

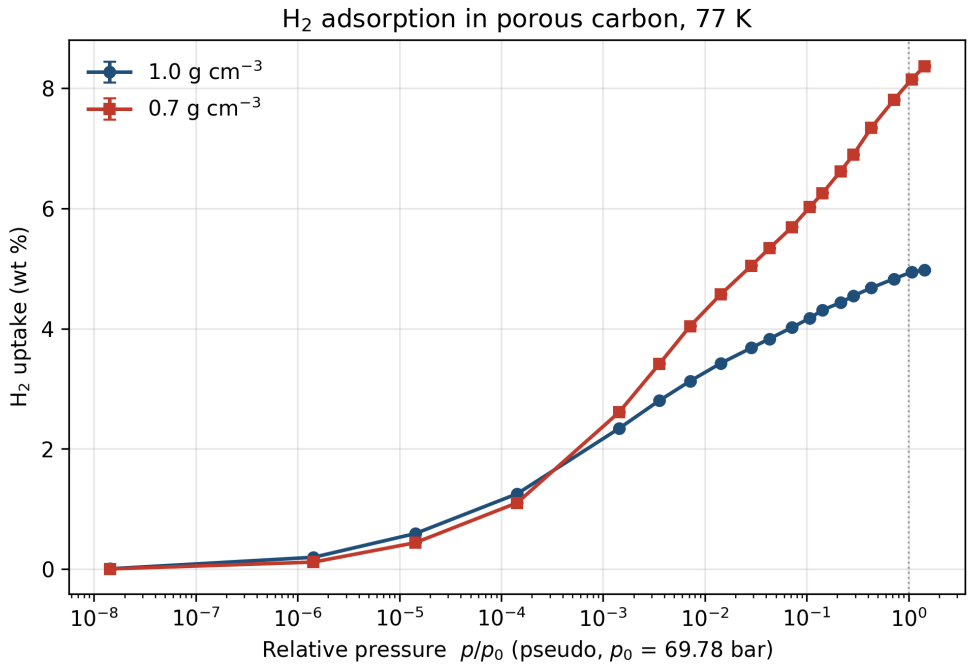


Figure 2 Hydrogen uptake at 77 K against relative pressure on a logarithmic axis, which is the only way to see seven decades at once. The dotted line marks $p/p_0 = 1$. Error bars are present but smaller than the symbols at most points.

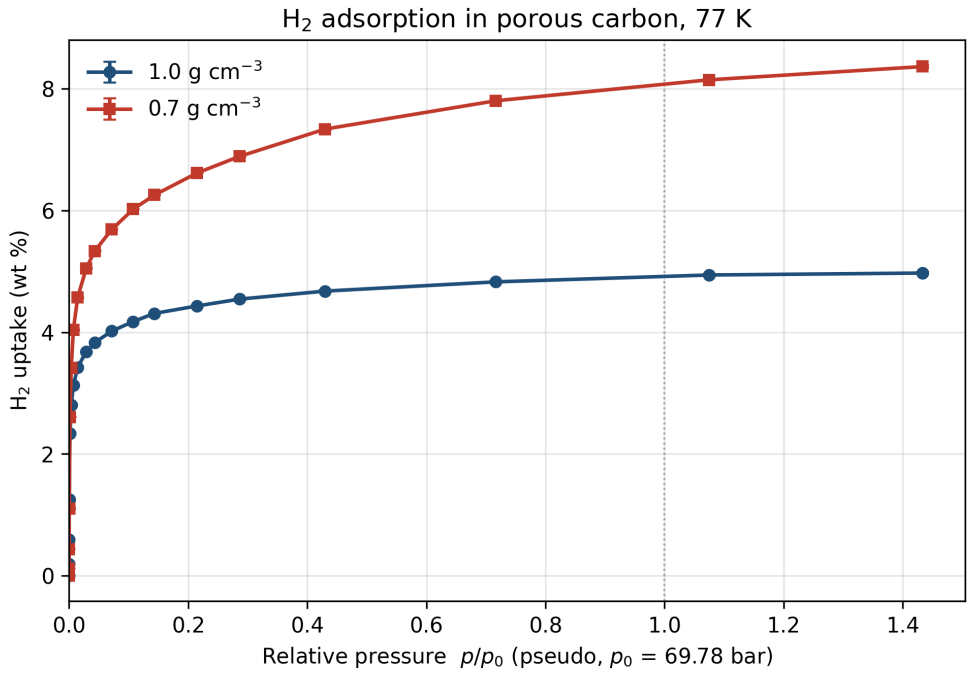


Figure 3 The same data on a linear relative-pressure axis. The curves flatten towards high pressure, which is what saturation looks like: the pores are close to full and extra pressure buys little.

The headline numbers are that at 100 bar the light carbon reaches **8.37 wt%** and the dense carbon **4.97 wt%** — so the light one holds about 68% more hydrogen per gram. But the two curves cross. At the lowest pressures the ranking is reversed, and the dense carbon is ahead by more than a factor of two.

> **Key Insight**
>
> Which carbon is "better" has no pressure-independent answer. Below roughly 0.05 bar ($p/p_0 \approx 7 \times 10^{-4}$) the dense carbon holds more per gram; above it, the light carbon does, and its lead widens all the way to 100 bar ($p/p_0 = 1.4$). Section 6 explains the mechanism.

4.2 Checking the runs are trustworthy

Before believing any of it, four things were checked, shown together in Figure 4.

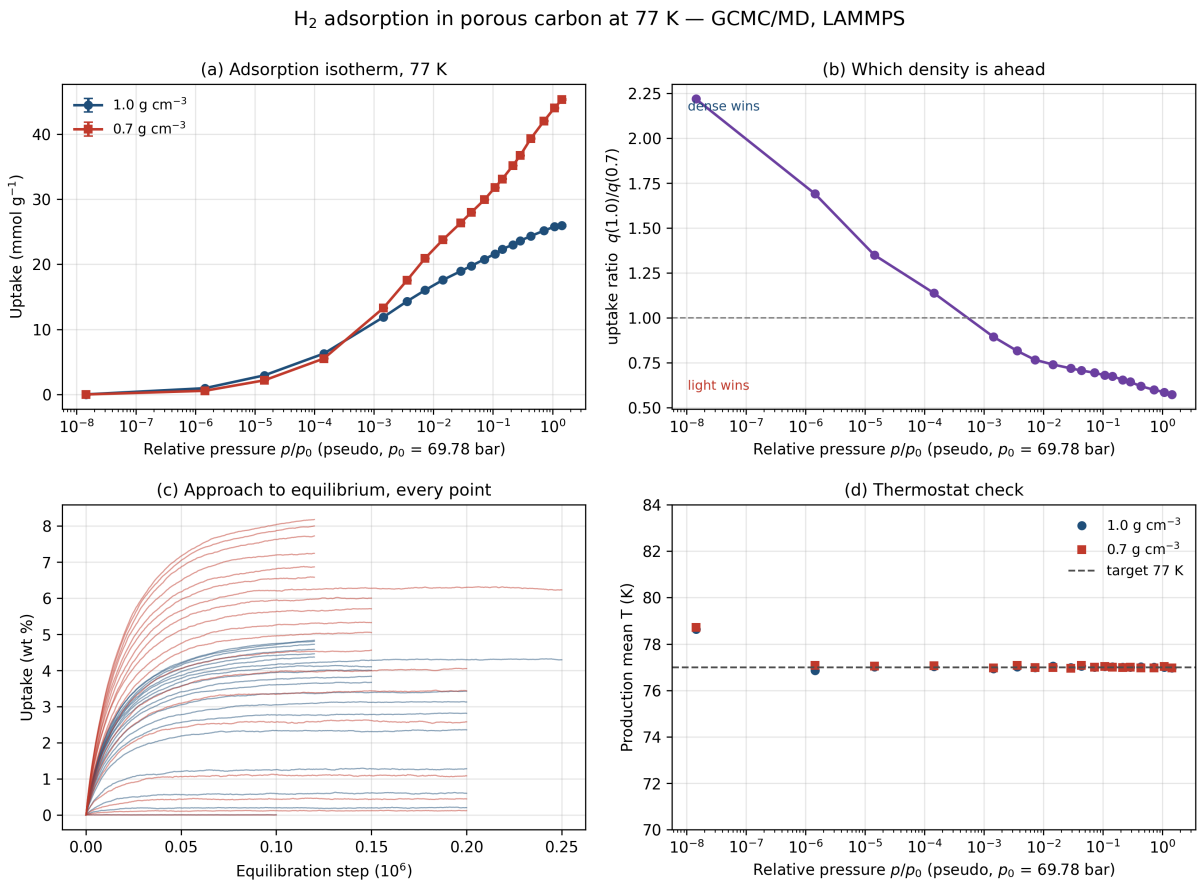


Figure 4 Quality checks on the hydrogen runs, all pressure axes relative. **(a)** The isotherms in mmol g^{-1}. **(b)** The ratio between the two densities, crossing 1.0 near $p/p_0 \approx 7 \times 10^{-4}$. **(c)** Molecule count during the settling phase for every pressure point — each one levels off well before measurement begins. **(d)** Average temperature at every point, sitting on the 77 K target.

Panel (c) matters most. It shows the number of molecules climbing steeply as hydrogen floods in, then flattening. Nothing from the climbing part is used; only once the count is flat does measurement start. Every run flattens comfortably in time, so no point is contaminated by the filling transient. Panel (d) confirms the thermostat is holding: every point sits on 77 K except the very lowest pressure, which contains only a handful of molecules and is therefore genuinely noisy rather than wrong.

4.3 Two ways of reporting the same thing

Uptake can be quoted as millimoles per gram, as weight percent, or as a volume of gas at standard conditions. These are the same measurement in different clothing, related by fixed conversion factors, and Figure 5 confirms the conversion is behaving.

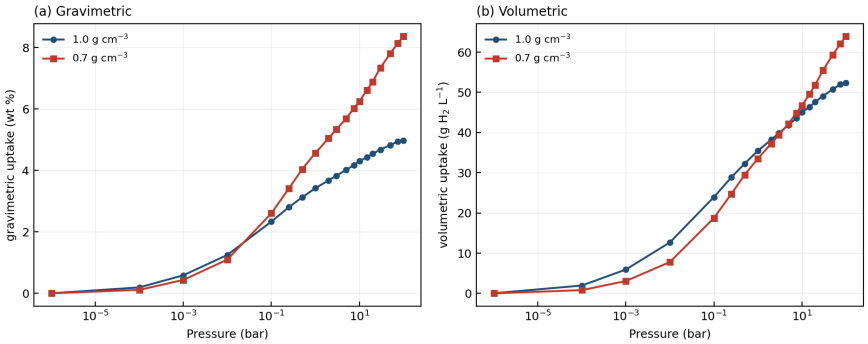


Figure 5 Gravimetric against volumetric uptake for hydrogen. The relationship is exactly linear, as it must be — this is a consistency check, not a result.

4.4 Where the hydrogen actually sits

Numbers tell you how much; pictures tell you where. Figure 6 slices a 12 Å slab through the middle of each simulation box and colours it by how much hydrogen is present.

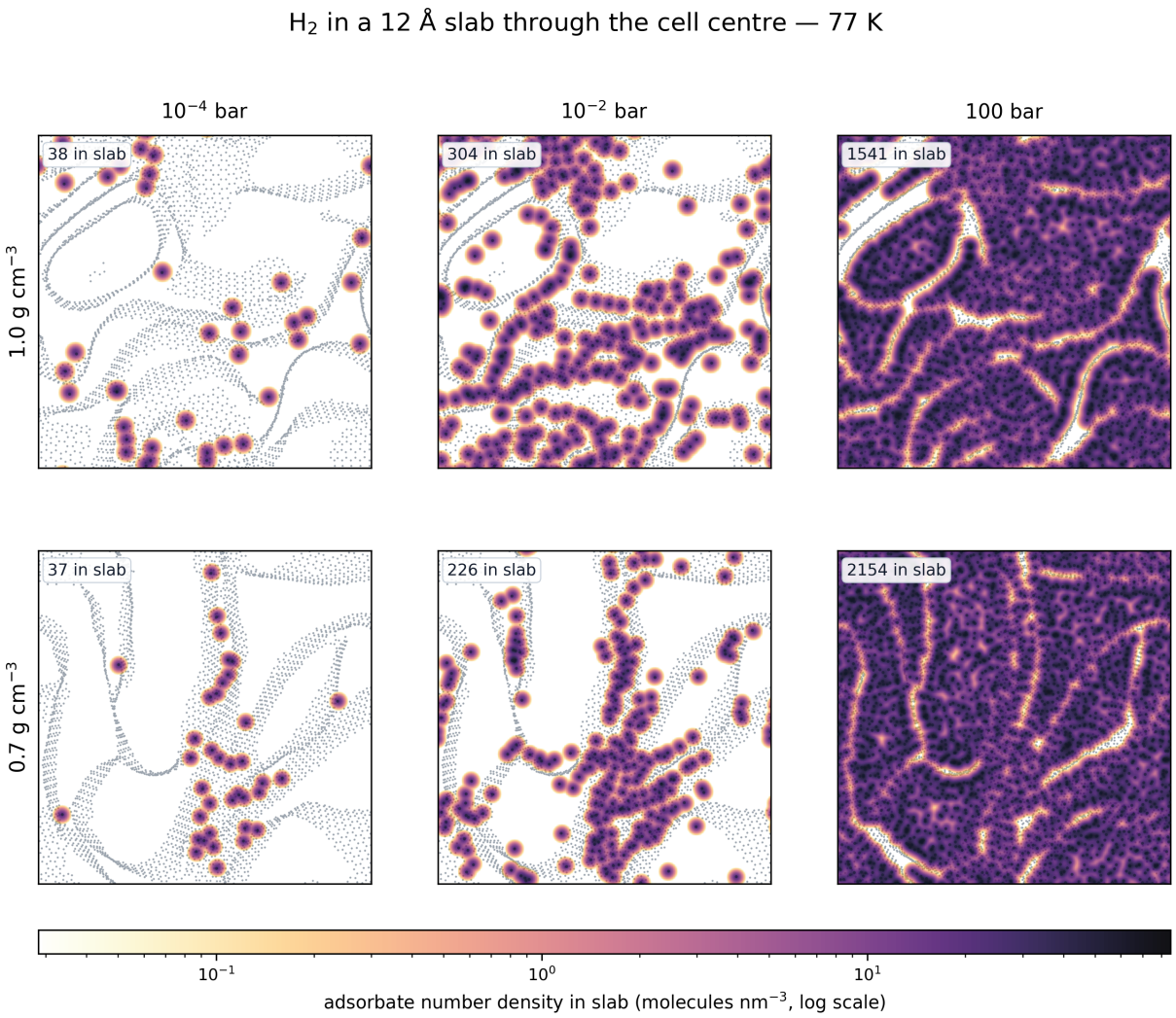


Figure 6 Hydrogen density in a slab through the centre of each cell. Grey dots are framework carbon; colour is hydrogen density on a shared logarithmic scale, so all six panels can be compared directly. At 10^{-4} bar only isolated strong-binding sites are occupied; by 100 bar the pore network is broadly full.

At the lowest pressure the hydrogen is not spread evenly — it sits in a scatter of isolated spots, always pressed against the carbon sheets, never in open space. Those are the strongest binding sites, the narrowest crevices, and there are more of them in the dense carbon. By 100 bar the picture is completely different: the pore network is filled throughout, and the light carbon, having more space to fill, holds more.

4.5 Full results

Table 3 Hydrogen uptake at 77 K. q in mmol g^{-1}; wt% is grams of H_2 per 100 g of loaded material. Relative pressure uses Dubinin's pseudo-saturation $p_0 = 69.78$ bar (see Section 6.1).

P (bar)	p/p_0	q 1.0	q 0.7	wt% 1.0	wt% 0.7
1e-06	1.43×10^{-8}	0.0205	0.0092	0.004	0.002
0.0001	1.43×10^{-6}	0.9713	0.5744	0.195	0.116
0.001	1.43×10^{-5}	2.9457	2.1825	0.590	0.438

P (bar)	p/p_0	q 1.0	q 0.7	wt% 1.0	wt% 0.7
0.01	1.43×10^{-4}	6.2891	5.5267	1.252	1.102
0.1	1.43×10^{-3}	11.8768	13.2765	2.338	2.607
0.25	3.58×10^{-3}	14.3166	17.5407	2.805	3.415
0.5	7.17×10^{-3}	16.0143	20.8940	3.127	4.042
1	1.43×10^{-2}	17.5883	23.7593	3.424	4.571
2	2.87×10^{-2}	18.9536	26.3734	3.680	5.048
3	4.30×10^{-2}	19.7596	27.9599	3.831	5.336
5	7.17×10^{-2}	20.7745	29.9246	4.020	5.689
7.5	1.07×10^{-1}	21.6155	31.7862	4.176	6.022
10	1.43×10^{-1}	22.3448	33.1014	4.310	6.256
15	2.15×10^{-1}	23.0093	35.1558	4.433	6.618
20	2.87×10^{-1}	23.6221	36.7158	4.546	6.892
30	4.30×10^{-1}	24.3379	39.2900	4.677	7.339
50	7.17×10^{-1}	25.1673	41.9919	4.829	7.805
75	1.07×10^{0}	25.7863	44.0076	4.941	8.149
100	1.43×10^{0}	25.9622	45.2891	4.974	8.366

5 Carbon dioxide capture at 273.15 K

Attention

This study is **unfinished**. Nine of seventeen pressure points are analysed for the dense framework and three for the light one (two further light-framework points finished after analysis and appear only in Figure 11). The points that were completed cover relative pressures from 10^{-4} to 10^{-2} — the lowest 1% of the intended range.

5.1 The pressure grid

Carbon dioxide at 273.15 K can be liquefied by pressure alone; its saturation pressure is $p_0 = 34.851$ bar. Adsorption science almost always plots against *relative* pressure p/p_0 rather than absolute pressure, because that is what determines how full the pores get.

When we converted the pressure grid, a pleasing thing emerged: the planned pressures are exactly $p/p_0 = 10^{-4}$ upwards in a 1, 2.5, 5, 7.5 sequence per decade. The nine completed points therefore span 10^{-4} to 10^{-2} — and the intended grid runs all the way to $p/p_0 = 1$, that is, 34.85 bar.

5.2 The isotherms

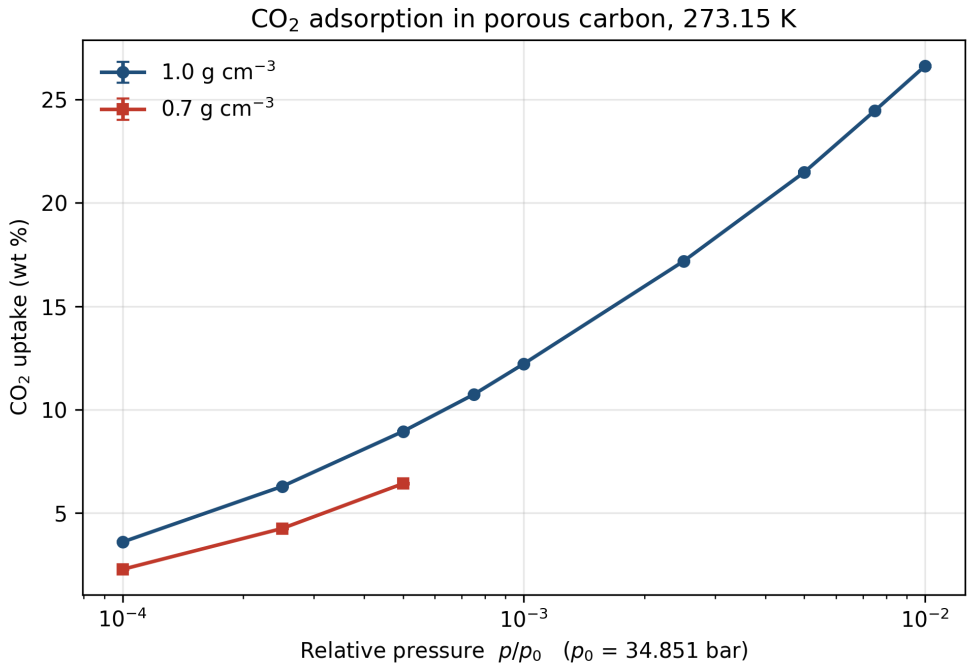


Figure 7 Carbon dioxide uptake at 273.15 K against relative pressure, logarithmic axis. Note the range: the whole plot spans $p/p_0 = 10^{-4}$ to 10^{-2}, the lowest 1% of the intended range. The light framework's series stops early because those runs are still queued.

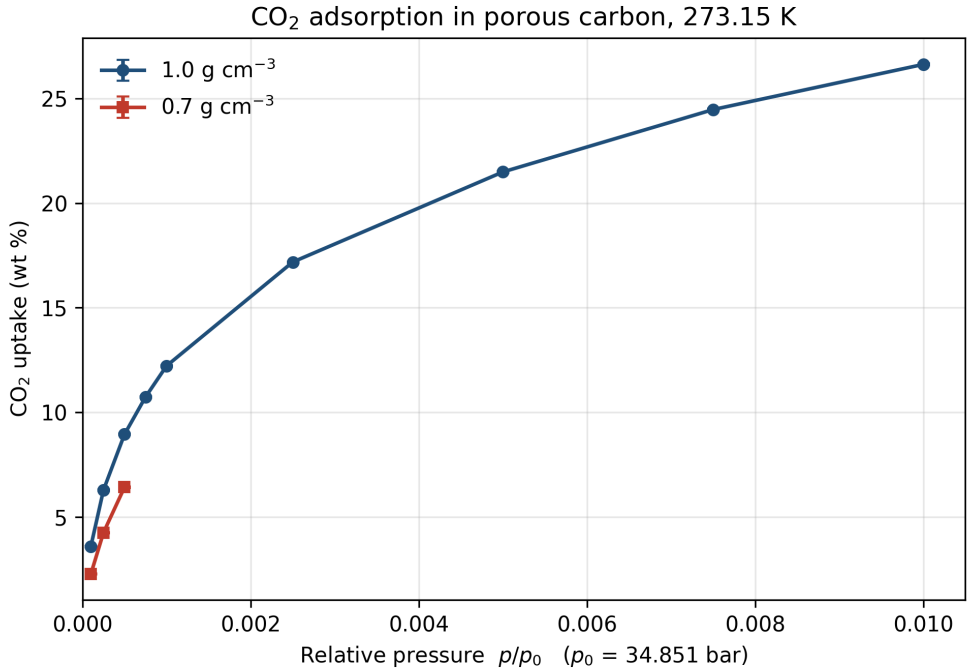


Figure 8 The same data on a linear relative-pressure axis. Unlike hydrogen, these curves are still climbing steeply where the data ends — this material is nowhere near full.

The dense framework reaches **8.25 mmol g^{-1}** (26.6 wt%) at 0.349 bar ($p/p_0 = 10^{-2}$) and is still rising. At every pressure both have reached, the dense framework holds more: the ratio runs 1.604, then 1.511, then 1.432. It is falling steadily, which is the same pattern hydrogen showed before its crossover.

5.3 Checking the runs

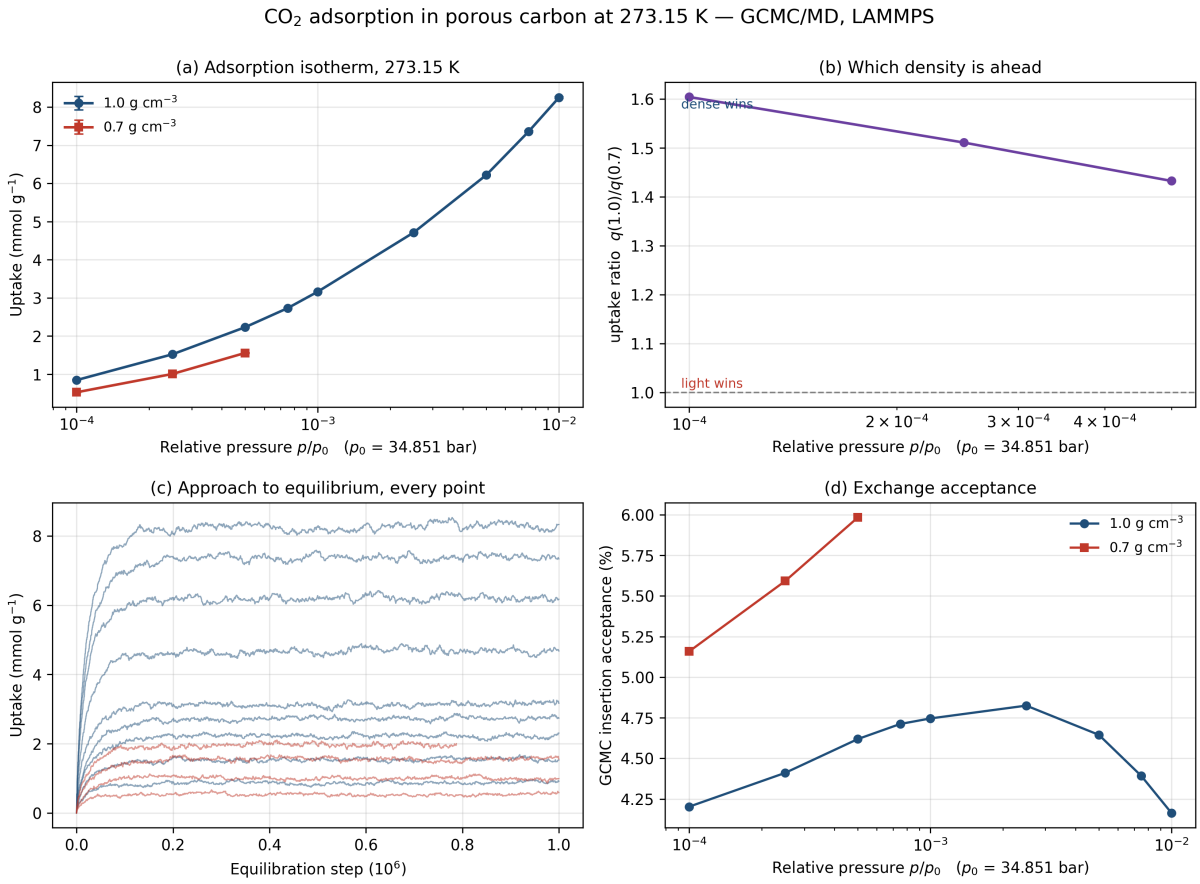


Figure 9 Quality checks on the carbon dioxide runs, all pressure axes relative. **(a)** The isotherms in mmol g^{-1}. **(b)** The ratio between the two densities — still well above 1.0, and falling, where the data stops. **(c)** Settling curves for every point, all flattening well before measurement begins. **(d)** GCMC insertion success rate, 4.2–6.0%.

The runs themselves are sound: every settling curve flattens, temperatures hold at 273.0–273.6 K against the 273.15 K target, and errors are below 1%. The problem is not run quality but run coverage — panel (b) makes that plain, since the ratio is still falling steadily when the data runs out.

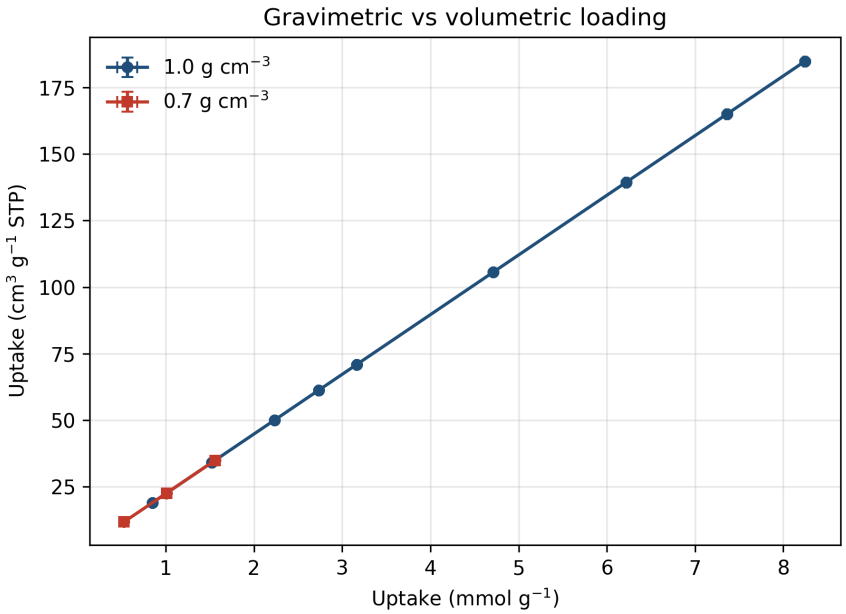


Figure 10 Gravimetric against volumetric uptake for carbon dioxide — again a linear consistency check.

5.4 Where the carbon dioxide sits

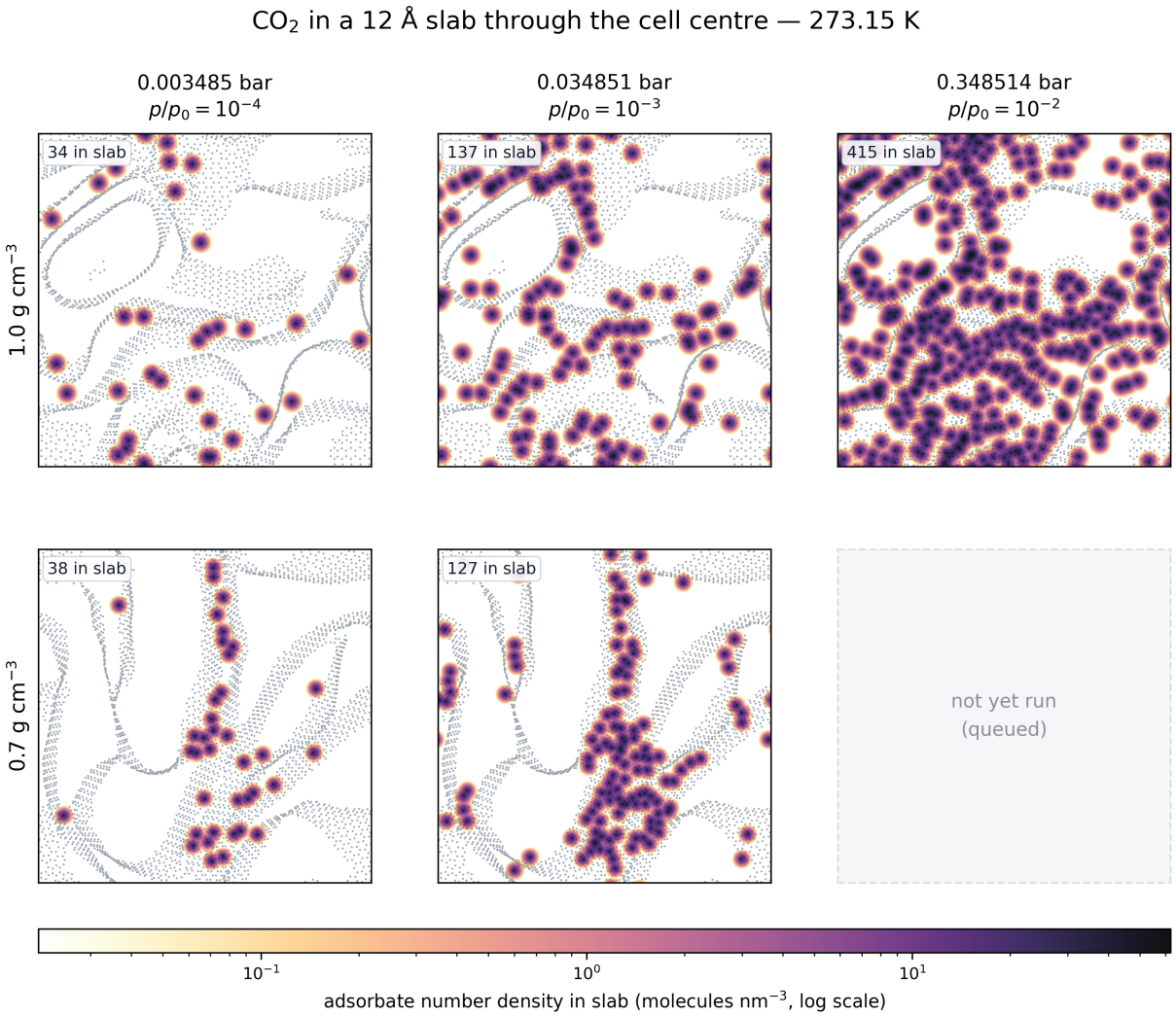


Figure 11 Carbon dioxide density in a 12 Å slab through the centre of each cell, on a shared logarithmic scale. Columns are one decade apart in relative pressure. The light framework's highest-pressure panel is marked as queued rather than quietly omitted.

The sequence is the clearest evidence in the report that this is pore *filling* rather than surface coating. At $p/p_0 = 10^{-4}$ the molecules sit in isolated pockets against the carbon sheets. By 10^{-3} those pockets have joined into threads following the sheets. At 10^{-2} the narrow regions are crowded — and yet the large open void near the top of the dense framework takes carbon dioxide only around its rim and stays empty in the middle. Wide spaces fill last.

5.5 Full results

Table 4 Carbon dioxide uptake at 273.15 K, for the points analysed. q in mmol g^{-1}. A dash means the run has not been analysed yet. p_0 = 34.851 bar.

P (bar)	p/p_0	q 1.0	q 0.7	wt% 1.0	wt% 0.7
0.003485	1.00×10^{-4}	0.8473	0.5282	3.595	2.272
0.008713	2.50×10^{-4}	1.5243	1.0088	6.286	4.251
0.017426	5.00×10^{-4}	2.2328	1.5588	8.947	6.419
0.026139	7.50×10^{-4}	2.7317	–	10.731	–
0.034851	1.00×10^{-3}	3.1629	–	12.218	–
0.087129	2.50×10^{-3}	4.7134	–	17.179	–
0.174257	5.00×10^{-3}	6.2188	–	21.487	–
0.261386	7.50×10^{-3}	7.3608	–	24.467	–
0.348514	1.00×10^{-2}	8.2463	–	26.627	–

Takeaway

The carbon dioxide isotherms are real and well converged, but they stop at $p/p_0 = 10^{-2}$. Any statement about saturation capacity, about the Henry's law limit, or about which density ultimately wins is an extrapolation, and is labelled as such throughout this report.

6 What the two gases show together

6.1 Both materials give Type I isotherms

The IUPAC classification sorts adsorption isotherms into six shapes, each pointing to a different mechanism [10]. Types I(a) and I(b) mean micropore filling. Type II means layer-by-layer growth on an open surface. Type III means the gas barely likes the solid. Types IV and V involve condensation in medium-sized pores. Type VI means growth in discrete layers.

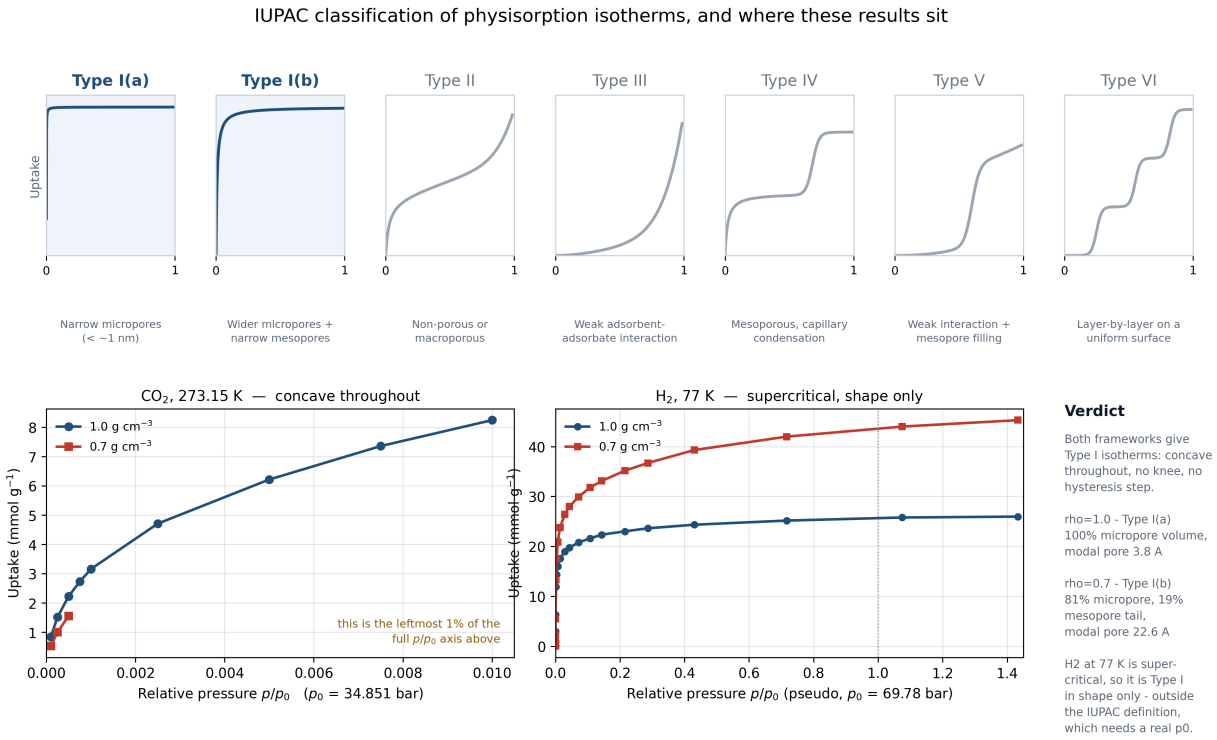


Figure 12 The six IUPAC isotherm types (Type I split into its two sub-types), with the two that match these materials highlighted. The lower panels show the measured isotherms on a *linear* relative-pressure axis, which is the axis the classification is defined on.

Every measured isotherm curves the same way — concave to the relative pressure axis at 100% of points, with no knee, no step, and no hysteresis. That rules out Types II through VI. Which sub-type applies then follows from the pore structure of Section 2: the dense framework, being 100% microporous, is **Type I(a)**; the light framework, with its 19% mesopore tail, is **Type I(b)**.

> **Note**
>
> Hydrogen at 77 K cannot strictly be given an IUPAC type at all. Hydrogen's critical temperature is 33.19 K, so at 77 K it is supercritical and has no true saturation pressure. We used Dubinin's pseudo-saturation pressure to put it on a comparable axis, and label those rows "I-like" rather than assigning a type.

6.2 How wide are the pores, really?

Because the isotherms are Type I, uptake can be treated as pores filling with liquid rather than surfaces being coated. That is what the Dubinin–Radushkevich equation describes [11]:

$$W = W_0 \exp\left[-\left(\frac{A}{\beta E_0}\right)^2\right], \qquad A = RT \ln\left(\frac{p_0}{p}\right).$$

Plotting $\ln W$ against A^2 turns this into a straight line whose intercept gives the total micropore volume W_0 and whose slope gives a characteristic energy E_0. A standard correlation then converts that energy into an average pore width [12].

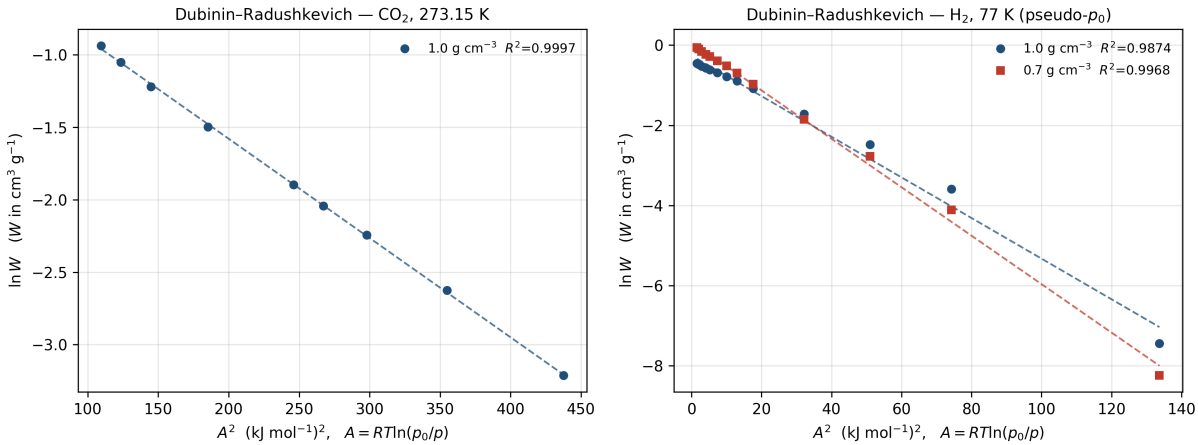


Figure 13 Dubinin–Radushkevich plots. Carbon dioxide on the dense framework is almost a perfect straight line. The hydrogen fits bend at small A^2 — the high-pressure end — which is the expected breakdown of this model for a supercritical gas.

Table 5 Dubinin–Radushkevich results. "Filled" is how much of the fitted micropore volume the highest measured point actually reached.

System	W_0 (cm^3g^{-1})	R^2	E_0 (kJ mol^{-1})	DR width (nm)	Geometric mode (nm)	Filled
CO_2, 1.0	0.811	0.9997	34.52	0.47	0.38	48%
CO_2, 0.7	*not fitted — fewer than four analysed points*					
H_2, 1.0	0.772	0.9874	26.13	0.73	0.38	96%
H_2, 0.7	1.084	0.9968	23.93	0.86	2.26	119%

Key Insight

The carbon dioxide fit on the dense framework has $R^2 = 0.9997$ and gives an average pore width of **0.47 nm**. The geometric analysis in Section 2, which never saw an isotherm, gives **0.38 nm**. Two completely independent methods — one thermodynamic, one purely structural — agreeing to within a tenth of a nanometre is the strongest internal check in this work.

The "Filled" column carries a practical warning. The completed hydrogen isotherm reaches 96% of its own fitted micropore volume: it has genuinely saturated. The carbon dioxide isotherm reaches only 48%. Despite looking as if it is levelling off on a logarithmic plot, the carbon dioxide run has filled under half the available pore volume, so any "maximum capacity" quoted from it is an extrapolation well beyond the data.

6.3 Why the two carbons swap places

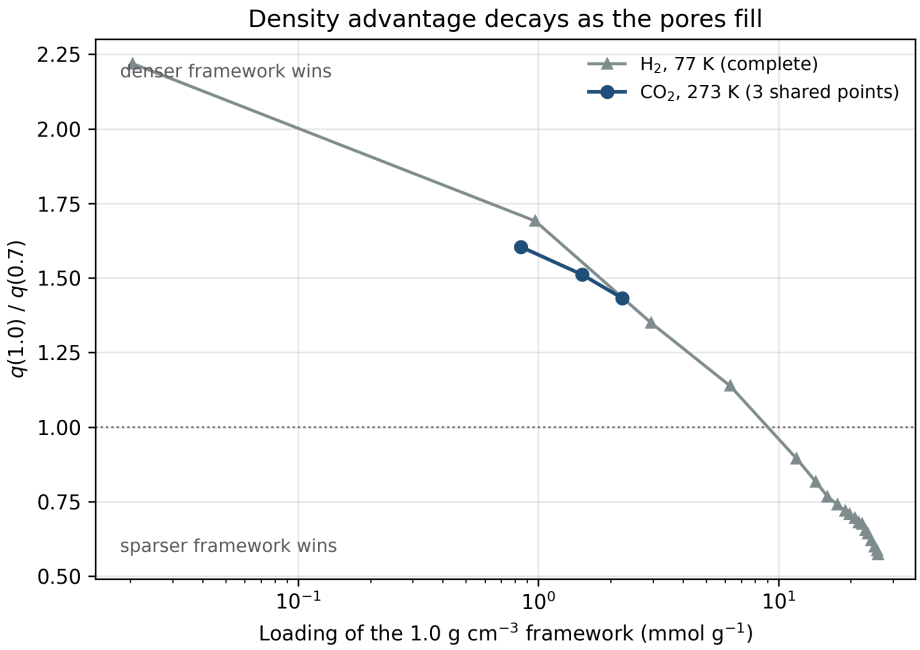


Figure 14 The dense framework's advantage, plotted against how much gas is loaded rather than against pressure. On this axis the three carbon dioxide points fall almost exactly on the completed hydrogen curve.

The mechanism is a straightforward trade-off between two things the frameworks have in different amounts:

- **Narrow pores bind harder.** A molecule in a tight crevice feels carbon walls on several sides at once, so it is held more strongly. The dense framework has far more of these — its most common pore is 3.8 Å across.
- **Wide pores hold more.** Once the strong sites are taken, what matters is sheer volume, and the light framework has 74% more of it.

So the dense framework leads when gas is scarce and loses when it is plentiful. The ratio falls steadily and crosses 1.0 at a loading of about 11.9 mmol g^{-1} for hydrogen.

Key Insight

Plotted against *loading* instead of pressure, the carbon dioxide points sit almost on top of the hydrogen curve. That suggests the crossover is governed by how full the pores are, not by pressure or by which gas it is. If that holds, carbon dioxide should cross over at roughly 9–12 mmol g^{-1} — and the highest completed CO_2 point reached 8.25. The crossover is one or two pressure points beyond where the runs stopped.

7 Closed porosity: the piece we did not finish

7.1 The problem

There is a flaw hiding in every GCMC simulation of a porous solid, and correcting it was part of the original project plan.

GCMC inserts molecules by proposing random positions anywhere in the box. It does not ask whether a molecule could physically have travelled there from outside. Real gas must diffuse in through a connected network of channels. If a pore is sealed off — surrounded entirely by carbon, with no opening wide enough to pass through — then a real experiment can never fill it, but the simulation fills it happily.

The consequence is that simulated uptake can be systematically too high, and the error is larger for materials with more sealed pores.

7.2 What we intended to do in LAMMPS

The plan was to identify the sealed pore space and exclude it from the simulation, so that computed uptake reflected only the porosity an experiment could actually reach. In practice that means classifying the void space into connected and isolated regions before the run, then either blocking insertions into the isolated regions or subtracting their contribution afterwards.

> **Attention**
>
> This was not implemented. Setting it up requires a pore-connectivity analysis feeding into the LAMMPS insertion routine, plus re-running every pressure point that had already been computed. With two months total and the isotherm campaign itself unfinished, there was no time. **Every uptake number in this report is therefore uncorrected for closed porosity.**

7.3 How much does it matter? A first measurement

Although the correction was never applied, we can now measure how large it would have been — which at least tells us whether it was worth doing.

The void space was divided into *open* regions, which connect continuously through the periodic boundary to form an infinite network, and *closed* regions, which form isolated pockets. The test is whether a pore, when the cell is tiled in space, joins up with its own neighbouring copies.

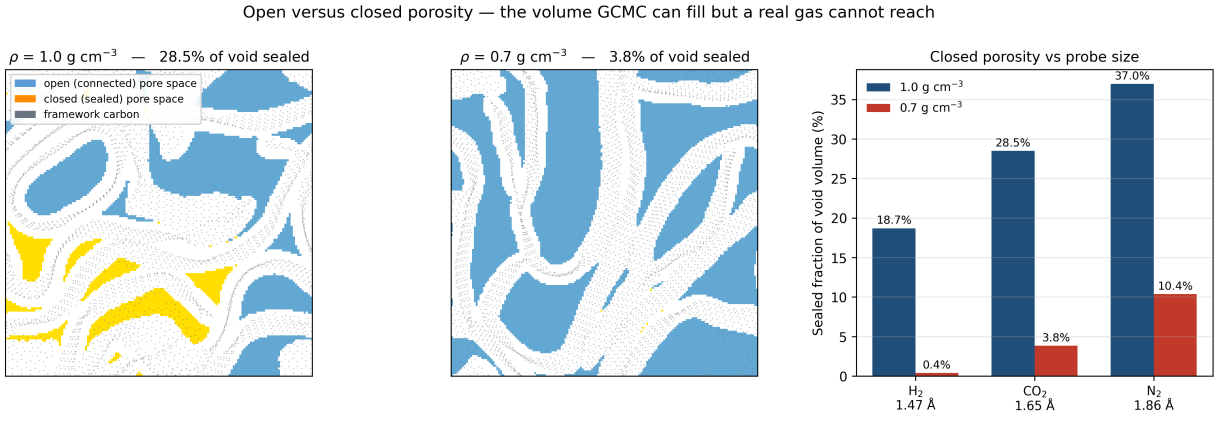


Figure 15 Open versus closed pore space. Blue is connected pore space a real gas could reach; orange is sealed pore space it could not. The right-hand panel shows how the sealed fraction grows with the size of the probing molecule — bigger molecules are shut out of more of the network.

Table 6 Sealed pore space, and the fraction of simulated uptake sitting inside it. Two probe sizes bracket the answer: a spherical CO_2 radius of 1.65 Å, and a narrower 1.30 Å representing the molecule threading a neck end-on. Reality lies between them.

	1.0 g cm^{-3}		**0.7 g cm^{-3}**	
Quantity	1.30 Å	1.65 Å	1.30 Å	1.65 Å
Void volume sealed	18.4%	28.5%	0.3%	3.8%
Simulated uptake sealed	24.0%	40.2%	14.2%	25.9%
Sealed void by probe size (H_2 1.47 Å, CO_2 1.65 Å, N_2 1.86 Å):				
H_2 probe	18.7%		0.4%	
CO_2 probe	28.5%		3.8%	
N_2 probe	37.0%		10.4%	

The result is larger than expected. Between a fifth and two fifths of the carbon dioxide the simulation placed in the *dense* framework sits in pores that a real gas could not reach. For the light framework the figure is roughly half that.

Takeaway

Closed porosity affects the dense framework about twice as strongly as the light one. That matters for the central comparison of this report: correcting for it would pull the dense framework's uptake down more than the light one's, which would shift the crossover in Section 6.3 to *lower* loading and narrow the dense framework's low-pressure advantage. The direction of the effect is clear even though the exact size is not.

This also offers the most likely explanation for something noticed earlier: the absolute carbon dioxide uptakes look high compared with what real activated carbons achieve at similar conditions. Some of that gap is probably sealed porosity being counted as usable.

8 Limitations

The carbon dioxide model has no charges. A CO_2 molecule has a strong quadrupole — an uneven spread of charge that governs much of how it interacts with surfaces. Our model leaves it out, and compensates with smaller, deeper interaction parameters than standard charged models use. This is the largest single approximation in the work. Absolute CO_2 capacities should be treated as provisional until checked against experiment or a charged model. The *comparison* between the two densities is more robust, because both use the same force field — though as Section 7 shows, closed porosity does not cancel out of that comparison.

Two thirds of the CO_2 campaign is unrun. Twenty pressure points remain queued, all at pressures higher than anything computed so far. Per-point cost rises steeply with pressure, from under four hours at the lowest point to sixteen hours at the highest so far, and the remaining points extend to $p/p_0 = 1$. Anyone continuing this work should check that the job time limit is generous enough before submitting them.

No Henry's law region was reached. The initial slope of an isotherm gives the Henry constant, from which binding energies and selectivities follow. Our lowest relative pressure, 10^{-4}, is still above that regime: the apparent slope falls monotonically from 243 to 24 mmol g^{-1}bar^{-1} across

the measured range. No Henry constant can be extracted, and no queued point goes lower, so this needs a dedicated low-pressure extension.

One temperature per gas. Everything here is at a single temperature for each gas. Isosteric heats of adsorption — the standard measure of binding strength — require at least two temperatures and so could not be computed.

Closed porosity is uncorrected. As set out in Section 7, and quantified there for the first time.

9 Conclusions

1. Both plastic-derived carbons are amorphous sp^2 networks, and both give **Type I** adsorption isotherms: gas fills narrow pores rather than coating surfaces. The dense framework is Type I(a), entirely microporous; the light one is Type I(b), with a mesopore tail.
2. **Neither density is better in general.** The dense carbon holds more per gram when gas is scarce, because it has more narrow strongly binding pores. The light carbon holds more once those pores are full, because it has 74% more volume. For hydrogen the swap happens at about 11.9 mmol g^{-1}; carbon dioxide appears to follow the same rule on a loading axis, but the runs stop just short of confirming it.
3. For practical hydrogen storage, which operates well above the crossover, the **0.7 g cm^{-3}** carbon is the better material, reaching 8.37 wt% at 100 bar against 4.97 wt%.
4. For carbon dioxide capture from dilute streams, which operates below the crossover, the **1.0 g cm^{-3}** carbon is ahead by a factor of about 1.4–1.5 per gram in the range measured.
5. Two independent methods — a thermodynamic fit and a direct geometric measurement — agree on an average micropore width near 0.4–0.5 nm for the dense framework, which is good evidence that both the structural model and the simulations are behaving sensibly.
6. **Closed porosity is a real and unresolved problem.** Between 18% and 29% of the dense framework's pore volume is sealed, holding 24–40% of the simulated carbon dioxide. Correcting for it was planned but not achieved within the two months available, and it should be the first task in any continuation.

Acknowledgements

This work was carried out under the supervision of **Carla De Tomas** and **Jorge Anderson Arboleda**, whose guidance shaped both the simulation design and the analysis. Calculations were performed on the UCL Young supercomputer through the MMM Hub, under allocation `KCL_De_Tomas`.

References

[1] Carla de Tomas, Irene Suarez-Martinez, and Nigel A. Marks. "Graphitization of amorphous carbons: A comparative study of interatomic potentials". In: *Carbon* 109 (2016), pp. 681–693. DOI: 10.1016/j.carbon.2016.08.024.

[2] Carla de Tomas, Irene Suarez-Martinez, and Nigel A. Marks. "Carbide-derived carbons for dense and tunable 3D graphene networks". In: *Applied Physics Letters* 112.25 (2018), p. 251907. DOI: 10.1063/1.5030136.

[3] Lev D. Gelb and K. E. Gubbins. "Pore Size Distributions in Porous Glasses: A Computer Simulation Study". In: *Langmuir* 15.2 (1999), pp. 305–308.

[4] Tina Düren et al. “Calculating Geometric Surface Areas as a Characterization Tool for Metal-Organic Frameworks”. In: *The Journal of Physical Chemistry C* 111.42 (2007), pp. 15350–15356.

[5] Anderson Arboleda-Lamus, Christian Forero, and Enrique Mejia-Ospino. “Molecular Dynamics Study of the Interactions of Graphene Oxide and Sandstone Surfaces”. In: *Langmuir* 42.5 (2026), pp. 3860–3869. DOI: 10.1021/acs.langmuir.5c05009.

[6] Aidan P. Thompson et al. “LAMMPS – a flexible simulation tool for particle-based materials modeling at the atomic, meso, and continuum scales”. In: *Computer Physics Communications* 271 (2022), p. 108171.

[7] Roger F. Cracknell. “Molecular simulation of hydrogen adsorption in graphitic nanofibres”. In: *Physical Chemistry Chemical Physics* 3.11 (2001), pp. 2091–2097.

[8] A. K. Rappé et al. “UFF, a full periodic table force field for molecular mechanics and molecular dynamics simulations”. In: *Journal of the American Chemical Society* 114.25 (1992), pp. 10024–10035.

[9] H. Flyvbjerg and H. G. Petersen. “Error estimates on averages of correlated data”. In: *The Journal of Chemical Physics* 91.1 (1989), pp. 461–466.

[10] Matthias Thommes et al. “Physisorption of gases, with special reference to the evaluation of surface area and pore size distribution (IUPAC Technical Report)”. In: *Pure and Applied Chemistry* 87.9-10 (2015), pp. 1051–1069.

[11] M. M. Dubinin. “The Potential Theory of Adsorption of Gases and Vapors for Adsorbents with Energetically Nonuniform Surfaces”. In: *Chemical Reviews* 60.2 (1960), pp. 235–241.

[12] F. Stoeckli and L. Ballerini. “Evolution of microporosity during activation of carbon”. In: *Fuel* 70.4 (1991), pp. 557–559.